Wind-tunnel tests of a tilt-rotor aircraft

G. Gibertini
giuseppe.gibertini@polimi.it
F. Auteri, G. Campanardi, C. Macchi and A. Zanotti
Dipartimento di Ingegneria Aerospaziale
Politecnico di Milano, Campus Bovisa
Milano, Italy

A. Stabellini
AgustaWestland, Helicopter System Design
Italy

ABSTRACT

A wide aerodynamic test campaign has been carried out on the tiltrotor aircraft ERICA at the Large Wind Tunnel of Politecnico di Milano by means of a modular 1:8 scale model in order to produce a dataset necessary to better understand the aerodynamic behaviour of the aircraft and to state its definitive design.

The target of the tests was the measurement of the aerodynamic forces and moments in several different configurations and different attitudes. The test program included some conditions at very high incidence and sideslip angles that typically belong to the helicopter-mode flight envelope and measurements of forces on the tail and on the tilting wings.

A large amount of data has been collected that will be very useful to refine the aircraft design. In general the aircraft aerodynamics do not present any critical problems, but further optimisation is still possible. From the viewpoint of drag in the cruise configuration, the sponsons of the landing gear seem to be worth some further design refinement since they are responsible for a 20% drag increase with respect to the pure fuselage configuration. On the contrary, the wing fairing has proved to work well when the aircraft longitudinal axis is aligned with the wind, providing just a slight drag increase.

Two other interesting aspects are the quite nonlinear behaviour of the side force for the intermediate sideslip angles as well as the noticeable hysteresis in the moment coefficient at very high incidence angles.

NOMENCLATURE

C_D	drag coefficient measured by main balance
C_{Dref}	drag coefficient measured by main balance for complete aircraft at zero incidence angle
C_{Dtilt}	drag coefficient measured by tilting wing balance
C_M	pitching moment coefficient measured by main balance
C_{Mref}	pitching moment coefficient measured by main balance for complete aircraft at zero incidence angle
C_{Mtilt}	pitching moment coefficient measured by tilting wing balance
C_N	yawing moment coefficient measured by main balance
C_{Nref}	maximum absolute C_N measured by main balance for complete aircraft with V2 fin
C_{Nt}	yawing moment coefficient measured by tail balance
GVPM	Politecnico di Milano Large Wind Tunnel
MB	main balance
RHW	right hand tilting wing
TB	tail balance
V1	small fin
V2	large fin
α	model incidence angle
β	model sideslip angle

Paper No. 3548. Manuscript received 26 February 2010, revised version received 21 September 2010 accepted 15 December 2010.

https://doi.org/10.1017/S0001924000005790

1.0 INTRODUCTION

The tiltrotor is at present one of the most promising projects in the aeronautical industry. Its unique capability to take off and land as a helicopter and to fly at high altitude and speed as an aeroplane makes the tiltrotor a suitable way to cope with the constant growth of transportation demand in the future, avoiding the congestion of the actual airport sites. In particular, its helicopter capabilities would enable narrow areas, at airport borders or near to the city centre, to be used for take off and landing. Therefore, a tiltrotor combining the cruise speed, comfort and range of present turboprops with vertical take off and landing capabilities of helicopters would probably become the reference vehicle in the very short-haul regional traffic aerospace market. Moreover the tiltrotor, since it provides all terrain accessibility, would be employed successfully also for search and rescue, emergency medical services, natural resources development support and service to isolated areas[1].

It took about 45 years of research to consolidate the vehicle architecture. In particular, the aerodynamic interactions between aircraft components have been investigated by wind tunnel tests on scale models, leading to successful improvements of the tiltrotor configuration concept [2]. Moreover, the analysis of wind tunnel tests results on full-span tiltrotor models allowed to evaluate the vehicle performance during the critical phases of its typical flight envelope that includes hovering, conversion from helicopter to aircraft mode and cruise[3].

Nowadays the full development of the first commercial tiltrotor (BA609[4]) is near to completion. The promising achievements encouraged the major European industries to concentrate their attention on the refinement of the architecture to improve productivity, consistency, safety and handling qualities of the vehicle.

The development of the European innovative tiltrotor aircraft design ERICA[5] (**E**nhanced **R**otorcraft **I**nnovative **C**oncept **A**chievement) has been the subject of several European Community funded research projects in the past years and received benefits from the previous experience acquired with the intensive wind tunnel campaigns carried out under EUROFAR[6,7]. European industries, research centres and universities have been involved in four different Critical Technology Programmes. The main goals of these projects were to develop and test the most critical components of the innovative aircraft such as the rotor hub and blades (DART)[8] and to design the complete drive system including nacelles and tilting wing mechanisms (TRISYD). Moreover, within the TILTAERO project[9] the complex flow field and noise related to the aerodynamic interaction among the tilting rotor and the other aircraft components such as fuselage, wing and tailplane, has been explored experimentally by means of wind tunnel tests at low and high speed regimes using a complete tiltrotor half-span mock-up and by numerical investigations (ADYN)[10].

The ERICA configuration presents two advanced features that enhance its performance with respect to the existing tiltrotors. A first innovation is the smaller rotor diameter that improves the vehicle performance in aeroplane mode allowing a higher speed, thanks to the higher efficiency of the propeller. The smaller rotor diameter assures a clearance between the rotor blade tip and the ground, even with the nacelles in aeroplane mode, allowing ERICA also to take off and land as a fixed wing aircraft.

The second innovative feature, that made the reduction of rotor diameter possible, is the capability of tilting the external half portion of the wing just below the rotors. Tilting the two half-wings reduces the interference between the rotor wake and the wing and the relative vertical forces, thus increasing the rotor efficiency in helicopter mode.

Recently in the framework of the European project NICETRIP, a wide wind tunnel test campaign on a modular 1:8 scale model of ERICA was performed in the Large Wind Tunnel of Politecnico di Milano. A 1:8 scale model, suitable to be employed in a medium size wind tunnel, was the best compromise between geometrical accuracy and costs.

The tests produced a comprehensive database suitable to provide the input to the performance prediction codes of the partners and a reference to validate CFD tools. The project was funded by the European Community's 6th framework programme. The present paper describes the wind tunnel activity performed on the scaled model and reports some selected results among the aerodynamic data set produced by the experiments.

2.0 EXPERIMENTAL SETUP

2.1 Wind Tunnel

The test campaign has been carried out in the 4m × 3·84m test section of the Large Wind Tunnel of Politecnico di Milano[11,12]. The GVPM is a 1·4MW closed loop wind tunnel driven by an array of 14 fans. The maximum wind velocity is 55ms^{-1} and the turbulence intensity is less than 0·1%.

The wind tunnel is equipped with a vertical pylon to support the model inside the test section as illustrated in Fig. 1(a). A hydraulic mechanism placed inside the pylon allows setting of the model incidence from –30° to 30°. The pylon is fixed over a rotating platform to set the sideslip angle from –180° to 180°.

(a) Model on the vertical pylon

(b) Model on very high incidence angle mounting

Figure 1. ERICA model setup in the wind tunnel.

https://doi.org/10.1017/S0001924000005790

(a) Tail balance (b) Tilting wing with clamps for internal balance calibration

Figure 2. Balances embedded in the model.

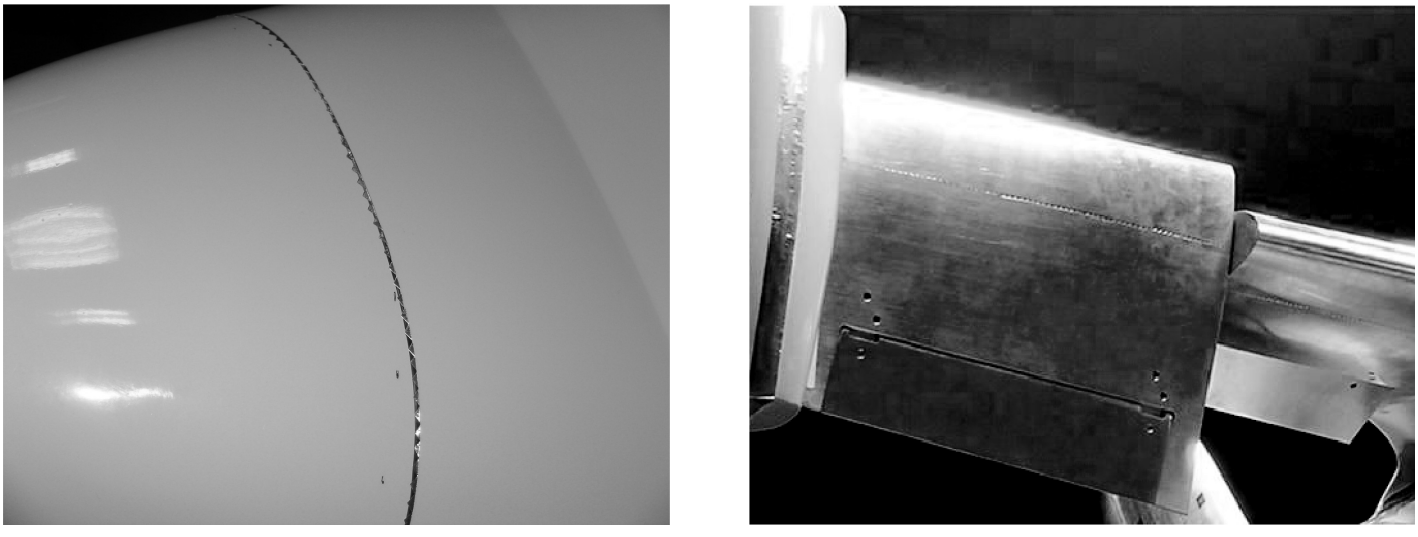

(a) Particular of the strip on the fuselage (b) Strip on tilting wing

Figure 3. Transition strips on the model.

A strut, composed of two 200mm diameter steel tube trunks, has been purposely built to install the pylon horizontally, as illustrated in Fig. 1(b).

2.2 The modular model

The modular construction of the model has been devised to allow testing of different configurations and to investigate the effects of each component separately. Tilting-wings and nacelles, as well as ailerons, rudder and elevator, could be mounted at different angles.

The model had an aluminium alloy internal frame to which the skin and aerodynamic surfaces could be fixed. The model wing span was 1·875m evaluated as the distance between the nacelle axes and the mass was of the order of 90kg, changing with each configuration. The model was equipped with the following balances:

- a six-component main balance inside the fuselage to measure the global aerodynamic loads and moments;
- a six-component tail balance to measure the loads and moments over the tailplane, see Fig. 2(a);
- two built-in, three-component balances to measure the loads over the tiltable wings, see Fig. 2(b).

The main balance, connecting the model frame to the pylon head, was attached to the wind-tunnel data acquisition system by means of a standard wire passing through the pylon itself. Differently, the partial balances of tail and wings were connected to an embedded data acquisition system communicating by a single USB cable. The embedded solution reduced the number of cables passing through the model support to only two: the data communication cable and the power supply cable. The good reliability and negligible electromagnetic noise warranted by the adopted system made this solution preferable with respect to a wireless one.

As the wind-tunnel Reynolds number was smaller than in the full-scale aeroplane mode flight condition, transition strips were positioned on the model surface, in particular on fuselage, wing, fin, tailplane and nacelles in order to force the boundary-layer transition, see Fig. 3. The transition strips were positioned where the transition was expected to be in cruise condition because this was the main focus of the test campaign. The transition position at full-scale cruise condition was estimated by means of numerical simulation with the CFD code VSAERO[13]. VSAERO was chosen since the transition position can be reliably predicted by an inviscid-viscous interaction approach. Adhesive tape transition strips were sized according to Braslow *et al*[14] and Cox[15].

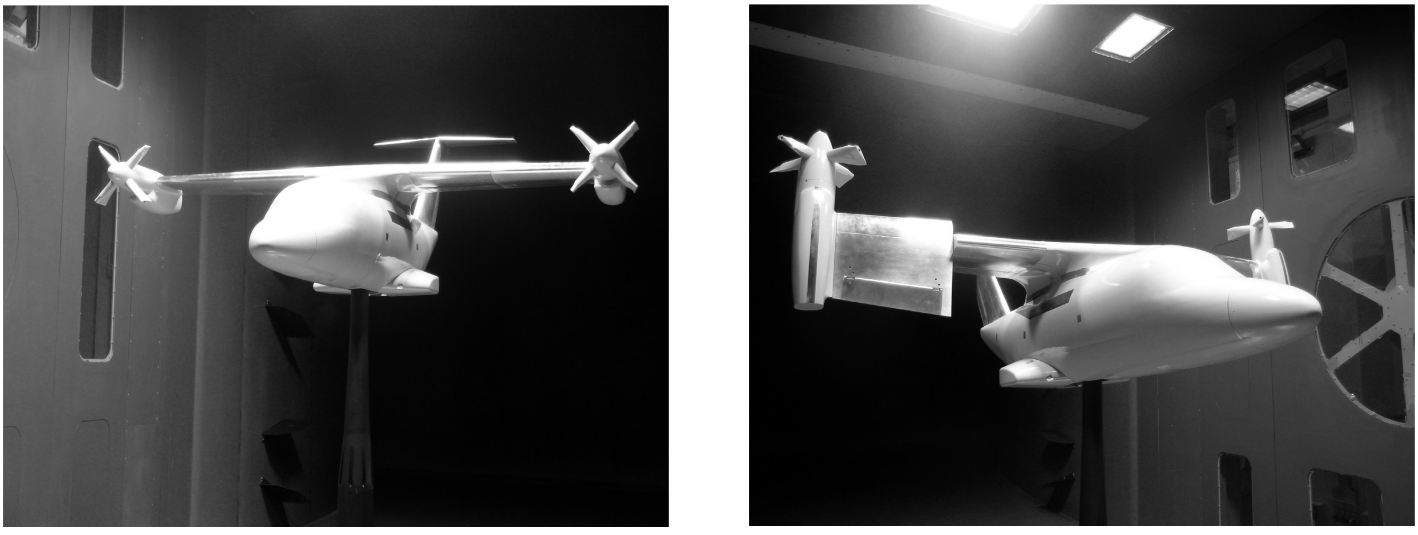

(a) Aeroplane mode (b) Helicopter mode

Figure 4. Complete ERICA model configuration.

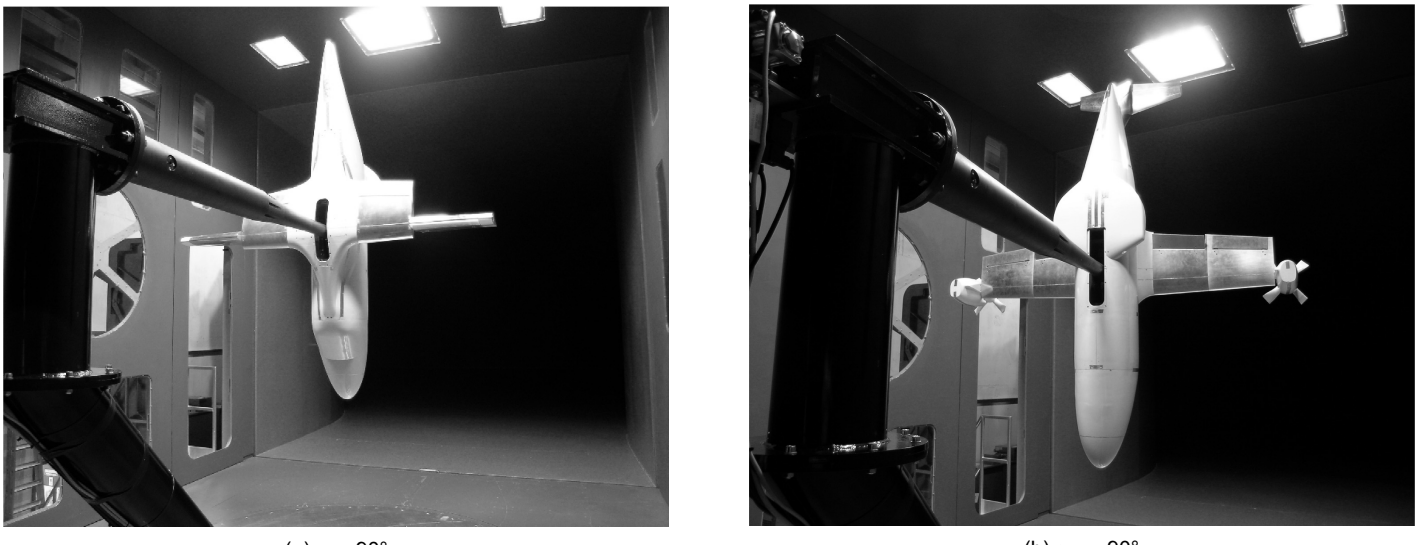

(a) α = 90° (b) α = –90°

Figure 5. ERICA model at very high incidence angle (in two different configuration).

3.0 TEST ACTIVITY

The wind-tunnel tests have been performed as angle of incidence sweeps at a fixed sideslip angle and sideslip angle sweeps at fixed incidence angles, using a step by step variation of the incidence and sideslip angle respectively. The wind-tunnel effects such as pylon interference, horizontal buoyancy in the test section, solid blockage, wake blockage and downwash have been evaluated as suggested in Barlow *et al*[16] and Maskell[18] and used to correct the measured aerodynamic coefficients. The aerodynamic coefficients measured for very high incidence angles have not been corrected for wind-tunnel effects, as the evaluation procedure is not assessed for such particular model settings.

Due to the high modularity of the model, incremental drag measurements, starting from the pure fuselage and successively adding a single component at a time, were performed. These tests allow the estimation of the drag contribution of each component which is necessary in the design phase to predict drag polars by a 'drag breakdown' procedure[16,17].

The tested configurations included the cruise flight condition in aeroplane mode and the conversion from aeroplane to helicopter mode with several combinations of nacelles and tilting wings settings, see Fig. 4. Moreover, the tested configurations included several settings of the control surfaces (flaps, ailerons, rudder and elevator) with the model in aeroplane mode. The wind-tunnel air velocity was 50ms^{-1} except for the tests with model configurations at very high tilted wings deflections. The wind-tunnel air velocity for these tests was limited to 40 or 30ms^{-1}, depending on the deflection angle, since the large deflection angle of the tilting wings produced heavy unsteady loads and, therefore large model oscillations.

The tests at very high incidence angles have been carried out during the last part of the activity with the setup described in Section 2.2. The test matrix included angles of incidence and angles of sideslip sweeps with the model in helicopter mode configuration at α = 90°, see Fig. 5(a) and tests with the model in the same configuration fixed at α = –90°, see Fig. 5(b). For very high model incidence angles both the fuselage and the wing behave as bluff bodies whose vortex shedding induced large oscillations of the model. Hence, for the sake of safety, the wind-tunnel air velocity was limited to 25ms^{-1} for these tests.

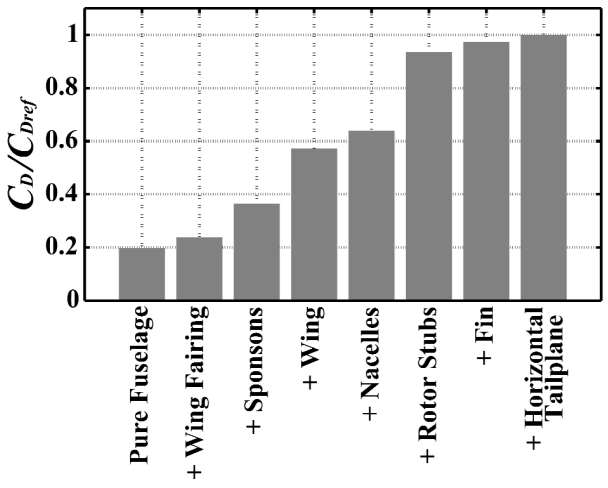

Figure 6. Drag analysis at α = 0° for drag breakdown tests.

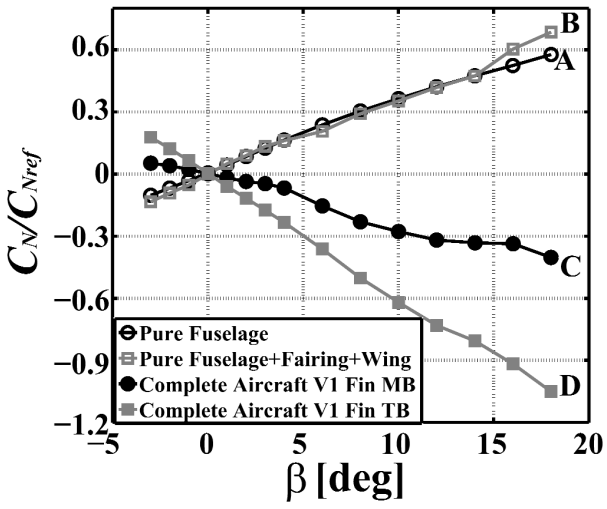

Figure 7. Comparison of $C_N - \beta$ curves: A) Pure Fuselage; B) Pure Fuselage + Fairing + Wing; C) Complete aircraft configuration with fin V1; D) Complete aircraft configuration with fin V1, tail contribution.

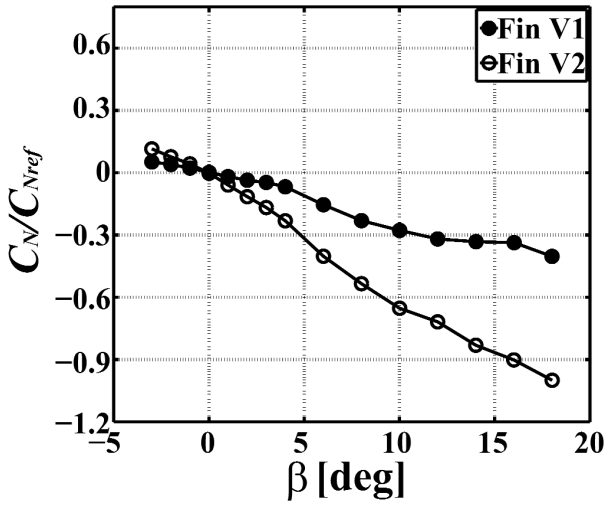

(a)

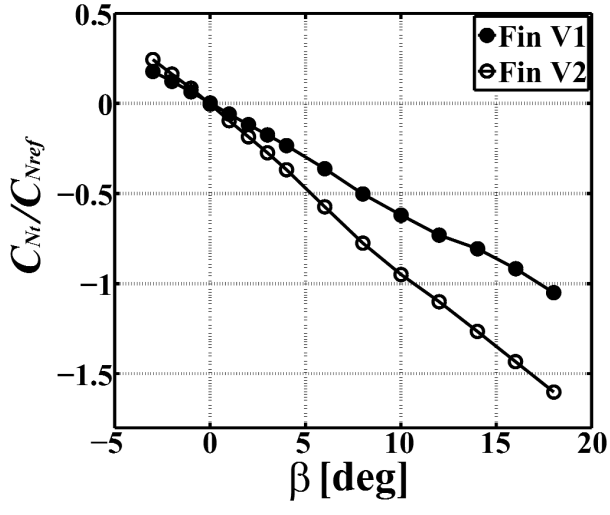

(b)

Figure 8. Comparison of $C_N - \beta$ and $C_{N_t} - \beta$ curves for complete model configuration with V1 and V2 fin.

4.0 RESULTS

A wide wind-tunnel test campaign has been carried out on the ERICA model. The experimental activity consisted of a total amount of 234 tests, including both angle of incidence and sideslip sweep tests. The large amount of results in terms of aerodynamic coefficients provided a comprehensive description of the aerodynamic behaviour of the aircraft both in aeroplane and in helicopter flight conditions.

A series of tests at α = 0° have been carried out for the drag breakdown analysis, starting with the pure fuselage and progressively adding the different model components, as the wing, the nacelles, the rotor stubs and the tailplane. These tests allowed the estimation of the drag increase produced by each individual component, highlighting the aircraft components that should be subject to design refinements to reduce the power for cruise flight.

As can be observed in Fig. 6, the drag increment due to the wing fairing is quite low. This experimental result validates the design solution for the fairing, conceived to integrate the fuselage with the very high wing necessary to avoid any interference between the rotor blades and the ground.

On the contrary, the impact of the sponsons on the drag seems to be quite high if compared, for instance, to the drag increase due to the nacelles and suggests that the actual configuration can be improved in this area.

The wind-tunnel data analysis suggested also the last adjustments in the aircraft sizing. The tail configurations tested included two fins with different surface, V1 and V2.

At the beginning of the model design activity the selected tail volume was considered adequate to meet the aircraft requirements in terms of control and stability.

Subsequently, in parallel with the model development, a more detailed handling qualities analysis showed the necessity to increase the tail volume to avoid a potential Dutch Roll instability problem.

At that point, it was decided to launch a new tail with an increased volume in addition to the initial one and it was planned to test both configurations in the wind-tunnel.

The analysis of the yawing moment of the complete aircraft with the smaller fin V1, measured in the β -sweep test, presents interesting results regarding the directional stability of the aircraft, see Fig. 7, where all the measured moments are referred to the position of the centre of gravity.

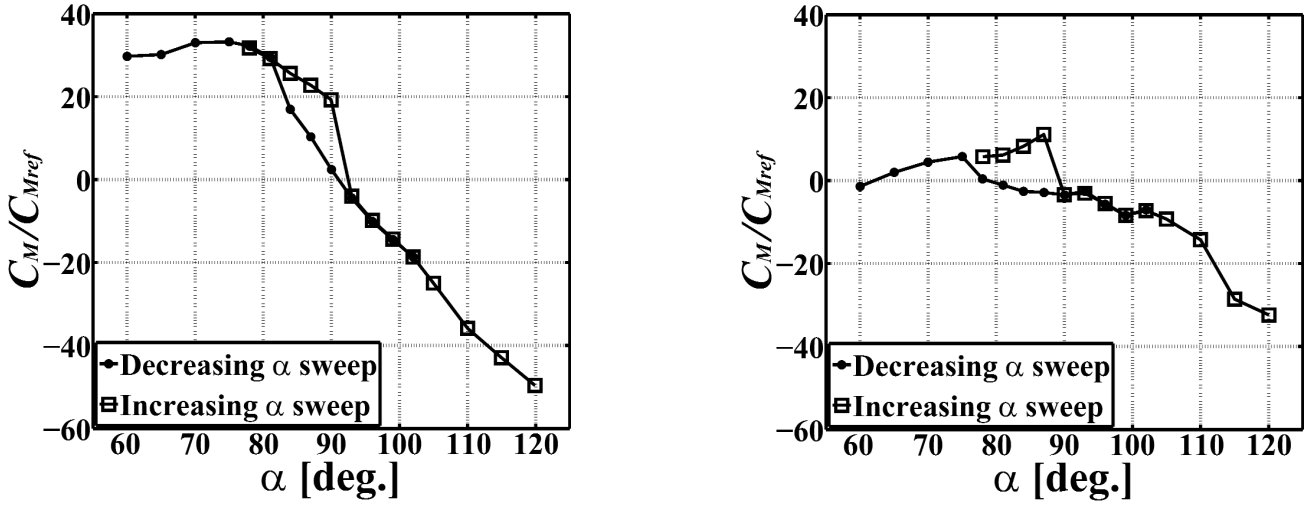

(a) Wing off configuration

(b) Winged configuration with tilting wings and nacelles set to 90°

Figure 9. C_M − α curve at very high incidence angles for two tail off configurations.

For low sideslip angles, the C_N − β curve of the tail off model (*B*) and that of the contribution due to the tail (*D*) are both linear. In particular, the curve slope for the tail contribution agrees well with theoretical prediction showing that the interaction between the fin and the wing fairing is not critical. As can be observed from Fig. 7, the curve slope for the complete aircraft configuration with fin V1 (*C*) decreases (increases in modulus) for sideslip angles higher than 4°. This effect can be explained by the same trend observed in the C_N − β curve of the pure fuselage (*A*).

For higher sideslip angles, the C_N − β curve for the complete configuration shows a remarkable slope increase (reduction in modulus). In particular, in the range between 12° and 16° the slope vanishes compromising the aircraft directional stability. This effect is mainly due to the wing and fairing aerodynamic behaviour, as confirmed by the curve *B* trend for the tail off configuration at the high sideslip angles. But it is also related to the slight aerodynamic nonlinearity of the tail behaviour due to the interference with the fuselage wake. The trend of curve *D* measured by the tail balance supports these considerations.

These results show that the combined effect of fin and fuselage with respect to the yawing moment does not produce a sufficiently high (negative) slope in the C_N − β curve to satisfy the flight mechanics requirements.

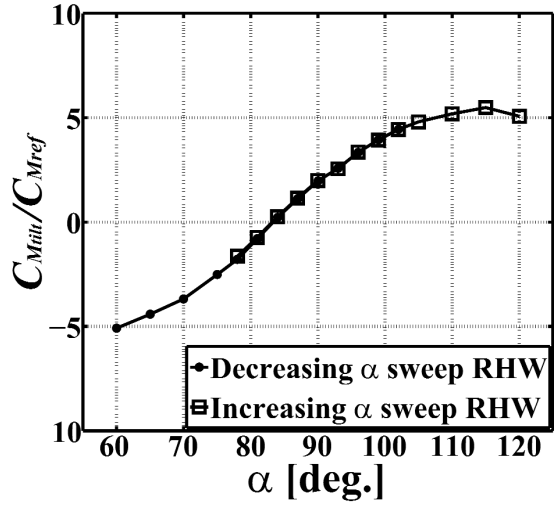

Figure 10. C_{Mtilt} − α curve at very high incidence angles for winged configuration with tilting wings and nacelles set to 90°.

Consequently, the tail volume has been redefined by both increasing the fin area and moving its position backward. As can be observed from Fig. 8, the C_N − β curve for V2 fin configuration still presents a quite nonlinear behaviour. By comparing Fig. 8(a) and 8(b) it becomes clear that such nonlinearity arises mainly from the contribution of the fuselage and wing, in fact it is more evident for the C_N − β curve than for the C_{N_t} − β curve. Nevertheless, due to the increased tail volume, the new fin satisfies the lateral stability requirements.

Figure 9 presents the pitching moment coefficient C_M measured at very high incidence angles for two different tail off configurations: (a) wing off model configuration with fuselage, wing fairing and sponsons and (b) winged configuration with tilting wings and nacelles set to 90°. This figure presents for each configuration the two C_M − α curves measured for decreasing and increasing α-sweeps to show the large hysteresis typical of these very high incidence angles.

The aerodynamic hysteresis is mainly due to a fuselage effect, as confirmed by the pitching moment coefficients measured on tilting wings. In fact, as can be observed in Fig. 10, the pitching moment coefficients measured by the tilting wing balance for winged configuration is not affected by hysteresis in proximity of α = 90°.

The aerodynamic hysteresis is recognisable also in the C_D − α curves presented in Fig. 11. An interesting aspect of the curves for winged configuration is the local minimum for α ~ 90°, see Fig. 11(b). This trend can be explained by the fact that for α = 90° the tilting wing is aligned with the free stream and therefore its drag reaches a local minimum. This minimum is quite sharp owing to the fact that in this condition the trailing edge acts as leading edge and therefore flow around the profile is prone to separation. In fact, the C_{Dtilt} − α measured by the right tilting wing balance for the same model configuration present a similar behaviour near to 90° incidence angle, see Fig. 12.

Finally, it is interesting to present, in Fig. 13, the drag coefficient C_D measured for both angle-of-incidence sweep and sideslip angle sweeps for the same two tail off model configurations. In order to improve readability of the curves, in this figure the average of increasing and decreasing sweeps are plotted within the hysteresis regions.

The minimum drag in the wing off configuration is obtained for a zero sideslip angle for α = 0° as expected, since the drag is minimum when the fuselage is aligned with the wind. For α = 90°, on the contrary, a rotation around the fuselage axis should not produce a

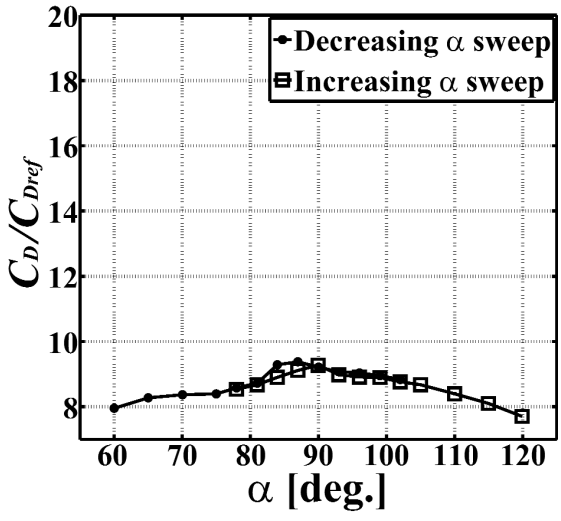

(a) Wing off configuration.

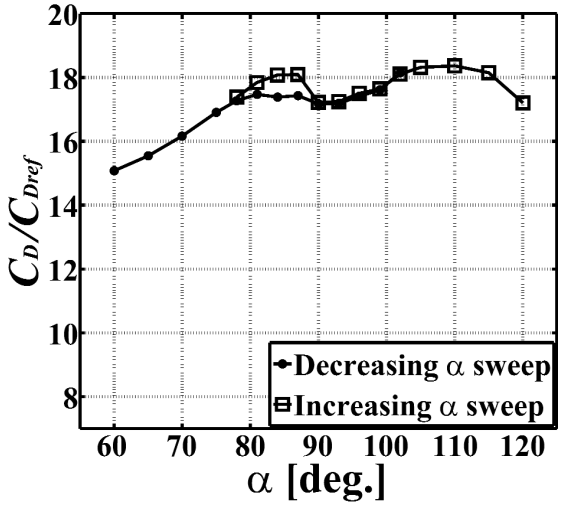

(b) Winged configuration with tilting wings and nacelles set to 90°.

Figure 11. $C_D - \alpha$ curves at very high incidence angles for two tail off configurations.

large effect for an almost axisymmetric fuselage, the observed drag increase with sideslip is therefore due to the wing fairing.

When the winged configuration is concerned, the plot of the drag coefficient reported in Fig. 13(b) shows a substantial increase in drag due to the presence of the fixed wing, for high incidence angles and due to the tilting wing, which is rotated by 90° in this configuration, at low incidence angles. For $\alpha = 0°$, near $\beta = 0°$ the drag is not a function of sideslip. This effect is due to the counteracting contributions of fuselage, whose drag increases with β and tilting wing, whose drag decreases with β. For $\alpha = 90°$, the contribution from the fixed wing decreases faster than the rate of drag increase due to the fairing, so that an overall decrease of drag with β is observed.

5.0 CONCLUSIONS

The ERICA tilt-rotor concept is quite unconventional with an unusual general layout and a quite wide flight envelope. In particular, the aircraft is characterised by tilting wings and by a quite high wing-fuselage interface position that requires a rather thick fairing. In the first phase of the NICETRIP European research program, a 1:8 scale model has been tested in the large wind tunnel at Politecnico di Milano to investigate the aerodynamic behaviour of this innovative project. The modularity of the model as well as the wind-tunnel equipment allowed the test of a wide set of configurations and attitudes, including very high incidence and sideslip angle conditions. The model was equipped with partial balances on the tiltable wings and on the tail that allowed the measurement of these single components contribution.

The results have been quite useful to verify the design solutions and to give indications for the final design improvements. For example, the incremental drag measurements, starting from the pure fuselage and successively adding a single component at a time, indicated the sponsons as the most critical point to be addressed for drag reduction, as they contribute a drag increase of 60% with respect to the pure fuselage.

The collected data show that an important hysteresis is present in the $C_M - \alpha$ curve at high incidence angles, order of 50% of the maximum value due to fuselage. The $C_D - \alpha$ also presents a hysteresis, but its amplitude is lower.

While the wing fairing contribution to the fuselage drag is 10% of the pure fuselage value in cruise conditions, for high incidence and sideslip angles its contribution becomes larger. For instance, for $\alpha = 90°$ and $\beta = 45°$ an increase ΔC_D of 170% with respect to C_{Dref} is observed.

More importantly, the interaction between the wing fairing and the fin seems to be at the origin of the nonlinear behaviour of the side force for sideslip angles greater than 4°, but this phenomenon requires a further investigation to be completely understood.

Moreover, the experimental activity allowed to improve tail efficiency by means of an increase of the tail volume in order to reach the expected performance in terms of lateral stability.

The test performed also provided suitable data input for the flight dynamic codes used by the NICETRIP Partners to evaluate the performance and the handling qualities of the ERICA tiltrotor.

In particular, specific software codes have been used to evaluate the aircraft stability properties during the conversion phase from helicopter to aeroplane mode.

Moreover the wind-tunnel test campaign performed on ERICA modular model provided structural loads information useful for the design of the larger 1/5 scale motorised model that is currently under development.

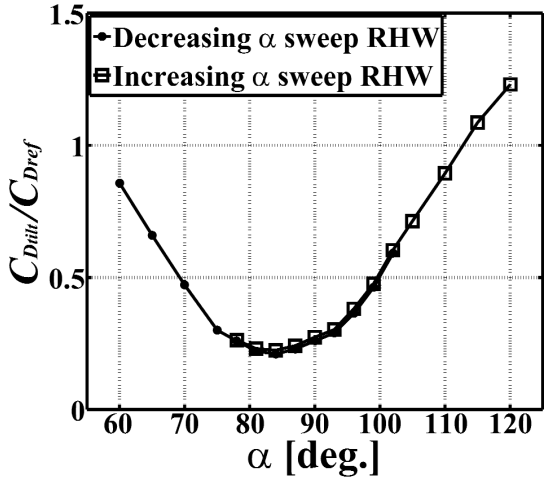

Figure 12. $C_{D_{tilt}} - \alpha$ curves at very high incidences angles for winged configuration with tilting wings and nacelles set to 90°.

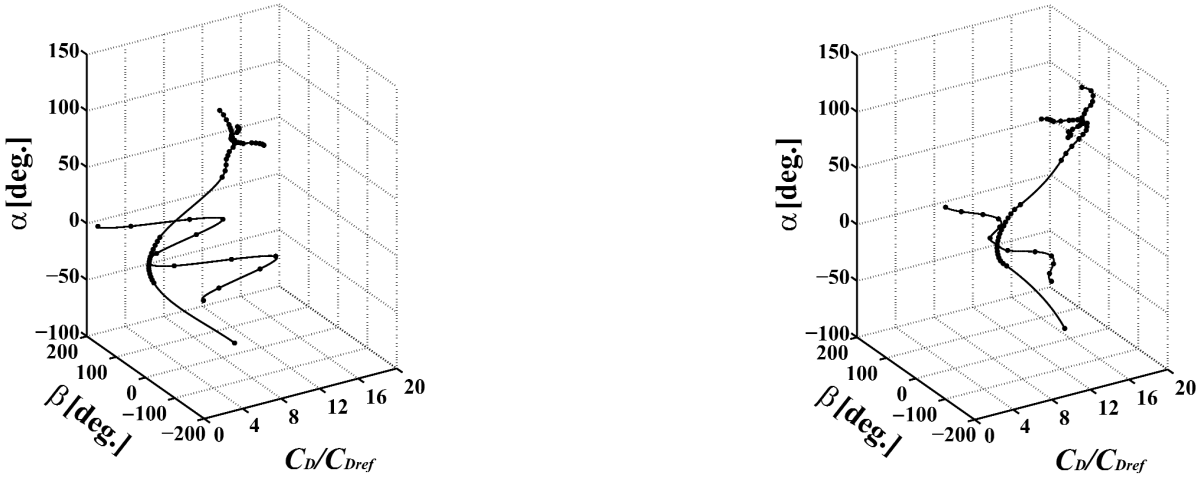

(a) Wing off configuration

(b) Winged configuration with tilting wings and nacelles set to 90°

Figure 13. $C_D - \alpha$ curve and $C_D - \beta$ curves for two tail off configurations.

REFERENCES

1. GAZDAG, D. and ALTONIN, L. Potential use of tiltrotor aircraft in Canadian aviation, NASA Technical Memorandum 102245, 1990.
2. MCVEIGH, M.A, GRAUER, W.K. and PAISLEY, D.J. Rotor/Airframe Interactions on Tiltrotor Aircraft, *J American Helicopter Society*, 1990, **35**, pp 43-51.
3. YOUNG, L.A., LILLIE, D., MCCLUER, M., YAMAUCHI, G.K. and DERBY, M.R. Insights into airframe aerodynamics and rotor-on-wing interactions from a 0·25-Scale tiltrotor wind-tunnel model, AHS International Aerodynamics, Acoustics and Test and Evaluation Specialists Conference, San Francisco, CA, USA, 23-25 January 2002.
4. BARBOUR, D.J. The BA609 tiltrotor aircraft: A new way to fly in the 21st century. Proceedings of Aircraft Symposium, 38th, pp 805-816, 2000.
5. ALLI, P., NANNONI, F. and CICALE, M. ERICA: the european tilt-rotor design and critical technology Projects, AIAA 2003-2515, AIAA International Air and Space Symposium and Exposition: The Next 100 Years, Dayton, Ohio, USA, 14-17 July 2003.
6. RENAUD, J., HUBER, H. and VENN, G. The EUROFAR program; A European overview on advanced VTOL civil transportation system, 17th European Rotorcraft Forum, Berlin, Germany, 23-27 September 1991.
7. BENOIT, B., BASSEZ, P. and GARDAREIN, P. EUROFAR rotor aerodynamic test, 18th European Rotorcraft Forum, Avignon (France), 15-18 September 1992.
8. BOTTASSO, C., TRAINELLI, L., ABDEL-NOUR, P. And LABO, G. Tiltrotor analysis and design using finite element multibody procedures, 28th European Rotorcraft Forum Paper, Bristol, UK. 17-20 September 2002.
9. VISINGARDI, A., DECOURS, J., KHIER, W. and VOUTSINAS, S. Code-to-code comparisons for the blind-test activity of the TILTAERO project, 31st European Rotorcraft Forum, Florence, Italy, 13-15 September 2005.
10. BIANCHI, E., RUSSO, A., KIESSLING, F., FERRER, R., DIETERICH, O., FROSONI, M., BAKKER, R., RIZIOTIS, V., PETOT, D. and LANZ, M. Numerical whirl-Flutter investigation of the European tiltrotor concept: current status and future prospects, 30th European Rotorcraft Forum, Marseilles, France, 14-16 September 2004.
11. DE PONTE, S., GASPARINI, L., GIBERTINI, G. and ZASSO, A. Optimisation of the Circuit Components for a Compact Civil-Aeronautical Wind-Tunnel, The Royal Aeronautical Society, *Wind Tunnels and Wind-Tunnel Test Techniques*, 1997, pp 1-8.
12. CAMPANARDI, G., GIBERTINI, G., POZZI, M.A. AND QUICI, M. La Camera di Prova Aeronautica della Galleria del Vento del Politecnico di Milano, Proceeding of XVII Congresso AIDAA, Rome, Italy, 15-19 September 2003 (in Italian).
13. VSAERO, Nonlinear Aerodynamic Software, User Manual, Analytical Methods, Inc.
14. BRASLOW, A.L., HICKS, R.M. and HARRIS, R.V. Use of Grit-Type Boundary-Layer- Transition Trips on Wind-Tunnel Models, NASA Tecnical Note, NASA TN D-3579, September 1966.
15. COX, R.A. Low speed, flat plate, carborundurum grit trip strip, AIAA 1980-868, American Institute of Aeronautics and Astronautics, International Meeting and Technical Display on Global Technology 2000, Baltimore, Md, USA, 6-8 May 1980.
16. BARLOW, J.B., RAE, W.H. and POPE, A. *Low-Speed Wind-Tunnel Testing*, John Wiley & Sons, 1999.
17. ROSKAM, J. Airplane design. Part VI: Preliminary calculation of aerodynamic, *Thrust and Power Characteristics*, DARCorporation, 2000.
18. MASKELL, E.C. A theory of blockage effects on bluff bodies and stalled wings in a closed wind tunnel, ARC R & M 3400, 1965.